Supporting Material

Cell Cytoskeleton and Tether Extraction

Bruno Pontes, Nathan B Viana, Leonardo T Salgado, Marcos Farina, Vivaldo Moura Neto and Herch Moysés Nussenzveig.

APPENDIX A. ANALYSIS OF THE RISING PART

In contrast with artificial vesicles, living cells react against stretch and tether pulling. To take the dynamical response of cells into account, we define the time-dependent viscoelastic complex modulus through its Fourier transform $\tilde{G}(\omega)$ by

$$\tilde{F}(\omega) = A(\theta)\tilde{G}(\omega)\tilde{x}(\omega), \tag{A1}$$

where $\tilde{F}(\omega)$ and $\tilde{x}(\omega)$ are, respectively, the Fourier transforms of the time-dependent force $F(t)$ applied to the cell membrane and of the corresponding length $x(t)$ of the extracted tether, and the geometric factor $A(\theta)$ is given by [1]

$$A(\theta) = 2\pi a f(\theta), \quad f(\theta) \equiv \left(\frac{9}{4\sin\theta} + \frac{3\cos\theta}{2\sin^3\theta} \right)^{-1} \tag{A2}$$

in which θ is the microsphere immersion angle in the cell (Fig. 3b). The geometric factor includes the effects both of bead translation and its rotation arising from the torque of the applied force [1,2].

To set up the initial value problem, we go over to Laplace transforms, with

$$\hat{G}(s) = \tilde{G}(is) \tag{A3}$$

so that Eq. 18 becomes

$$\hat{F}(s) = A(\theta)\hat{G}(s)\hat{x}(s) \tag{A4}$$

and Eq. 10 yields

$$\hat{x} = \frac{V}{s^2} - \Delta\hat{\rho}(s) \tag{A5}$$

From Eq. A4, we also have

$$\hat{F}(s) = k_{\perp}\Delta\hat{\rho}(s). \tag{A6}$$

Combining Eqs. (21), (22) and (23), we finally get

$$\Delta\hat{\rho}(s) = \frac{V}{s^2}\left[1 + \frac{k_\perp}{A(\theta)\hat{G}(s)}\right]^{-1}. \tag{A7}$$

Equivalently, from Eq. (22),

$$\hat{x}(s) = \frac{V}{s^2}\left[1 + \frac{A(\theta)}{k_\perp}\hat{G}(s)\right]^{-1}. \tag{A8}$$

This is a general result for the Laplace transform of the time-dependent displacement from equilibrium versus that of the viscoelastic frequency-dependent complex modulus. Inverting it, we determine the shape of the rising part of the response curve. To proceed further, we need a model for the response function.

Universality

The behavior of $\tilde{G}(\omega)$ as a function of ω has been investigated by a variety of techniques, including optical magnetic twisting cytometry [3,4] and oscillating optical tweezers [5,6]. Remarkably, a quasi-universal power-law behavior was found, holding for different cell types and species [7,8]. As stated in a recent review [8], such behavior holds over a wide range of experimental conditions, whether the cell is probed locally or on the whole cell level. The law may be written as [5]

$$\tilde{G}(\omega) = G_0\left(\frac{i\omega}{\omega_0}\right)^\alpha + i\omega\mu \tag{A9}$$

where G_0 and ω_0 are scaling factors, μ is an additive Newtonian viscosity, relevant at frequencies above 30 Hz, and the exponent α is typically of the order of 0.2.

As an illustration of tether extension dynamics, let us assume that the viscoelastic frequency-dependent complex modulus may be represented by Eq. A9, and let us initially neglect viscosity. Then, substituting the power-law term into Eq. A8, and introducing the notation

$$B \equiv \frac{k_\perp \omega_0^\alpha}{G_0 A(\theta)} \tag{A10}$$

we get

$$\hat{x}(s) = \frac{VB}{s^2}\left(\frac{1}{B + s^\alpha}\right). \tag{A11}$$

The inversion of this Laplace transform is performed in Appendix B. The result is given by Eq. B5:

$$x(t) = \frac{BV}{\pi}\sin(\pi\alpha)\int_0^\infty \frac{u^\alpha\left(e^{-ut} - 1 + ut\right)}{\left[u^{2\alpha} + 2B\cos(\pi\alpha)u^\alpha + B^2\right]}\frac{du}{u^2}. \tag{A12}$$

The integral converges sufficiently fast at both ends so that standard numerical integration programs can be applied.

In our experiments, V = 0.076±0.005 μm/s, measured values for the bead immersion angle θ are given in Fig. 4. Thus, the unknowns in Eq. A10 are the power-law exponent α and the modulus G_0 at the normalization frequency ω_0, which is usually taken to be 1 Hz.

Typical values of α found for a variety of cell types [1] range from 0.15 to 0.30. An example of a fit to Eq. A10 for control cells, taking the average value <α> = 0.22, is shown in Fig. S1, yielding the value G_0 = 977 Pa. Note that the fit skips a region near the origin that might still be contaminated by sliding over the membrane (see also Fig. 2d). From N = 32 such fits, we get $\langle G_0 \rangle$ = 1000 ± 10% Pa, consistent in order of magnitude with the $\langle G_0 \rangle$ values quoted in [1]. Corresponding fits including the extremes of the range of variation for α are: $\alpha = 0.15 \rightarrow \langle G_0 \rangle = 720 \pm 10\%$ Pa; α=0.30 $\rightarrow$ $\langle G_0 \rangle = 1500 \pm 10\%$ Pa.

Inclusion of the Newtonian viscosity term in Eq. A9, with reasonable numerical values, is consistent with the Laplace transform inversion performed in Appendix B and does not significantly affect the model parameter values found above.

APPENDIX B. INVERSION OF THE LAPLACE TRANSFORM

It follows from the theory of Laplace transforms [9] that the inverse Laplace transform of Eq. A8 is

$$x(t) = VB\int_0^t du\int_0^\tau dv f(v), \tag{B1}$$

where

$$f(v) \equiv \mathcal{L}^{-1}\left(\frac{1}{B + s^\alpha}\right) \tag{B2}$$

and $\mathcal{L}^{-1}$ stands for the inverse Laplace transform, given by

$$f(v) = \frac{1}{2\pi i}\int_{\delta - i\infty}^{\delta + i\infty}\frac{\exp(vs)}{B + s^\alpha}ds, \tag{B3}$$

with δ so chosen that all singularities lie to the left of the path of integration.

We cut the *s* plane along the negative imaginary axis, with $|\arg s| \le \pi$. The denominator has no zeros in the cut plane, since $0 < \alpha < 1$, so that we may take $\delta = 0$. The integrand tends to zero uniformly as $|s| \to \infty$ in the left half-plane, so that, by Jordan's lemma [10], the integral along the imaginary axis may be deformed into a half-circle at infinity in this half-plane, transforming it into an integral around the cut. The result is

$$f(v) = \frac{\sin(\pi\alpha)}{\pi} \int_0^\infty \frac{y^\alpha \exp(-vy)}{y^{2\alpha} + 2B\cos(\pi\alpha) y^\alpha + B^2} dy \,. \tag{B4}$$

Substituting this result into Eq. A1, we finally get

$$x(t) = \frac{BV}{\pi} \sin(\pi\alpha) \int_0^\infty \frac{u^\alpha \left(e^{-ut} - 1 + ut\right)}{\left[u^{2\alpha} + 2B\cos(\pi\alpha) u^\alpha + B^2\right]} \frac{du}{u^2} \tag{B5}$$

REFERENCES

[1]. M.Balland D, N., Icard, D., Féréol, S., Asnacios, A., Browaeys, J., Hénon, S., and Gallet, F. 2006. Power laws in microrheology experiments on living cells: Comparative analysis and modeling. Phys Rev E. 74:021911-1 - 021911-17.

[2]. Laurent VM, S. Hénon, E. Planus, R. Fodil, M. Balland, D. Isabey, and F. Gallet 2002. Assessment of mechanical properties of adherent living cells by bead micromanipultion: comparison of magnetic twisting cytometry vs optical tweezers. J Biomech Eng. 24:408-421. The last term within parentheses in Eq. A2 represents the torque contribution. It is not expected to be present in our experiments, but it has been kept in order to enable comparison of our fitting parameters to those given in [1].

[3]. Fabry B, G. N. Maksym, J. P. Butler, M. Glogauer, D. Navajas, and J. F. Fredberg 2001. Scaling the microrheology of living cells. Phys Rev Lett. 87:148102-1 - 148102-4.

[4]. Fabry B GNM, J. P. Butler, M. Glogauer, D. Navajas, N.A. Tabackm E. J. Millet, and J. F. Fredberg 2003. Time scale and other invariants of integrative mechanical behavior in living cells. Phys Rev E. 68:041914-1 - 041914-18.

[5]. Wei M-T, A. Zaorski, H. C. Yalcin, J. Wang, M. Hallow, S. N. Ghadiali, A. Chiou, and H.D. Ou-Yang 2008. A comparative study of living cell micromechanical properties by oscillatory optical tweezers. Opt Express. 16:8594-8603.

[6]. Trepat X, L. Deng, S. S. An, D. Navajas, D. J. Tschumperlin, W. T. Gerthoffer, J. P. Butler, and J. J. Fredberg 2007. Universal physical responses to stretch in the living cell. Nature. 447:592-596.

[7]. Trepat X, G. Lenormand, and J. J. Fredberg 2008. Universality in cell mechanics. Soft Matter. 4:1750-1759.

[8]. Stamenovic D. 2008. Rheological behavior of mammalian cells. Cell Mol. Life Sci. 65:3592-3605.

[9]. Widder, D. V. 1941, The Laplace Transform. Princeton: Princeton University Press.

[10]. Whittaker, E. T., and G. N. Watson 1952. A Course of Modern Analysis, 4th ed. Cambridge: Cambridge University Press.

FIGURE AND MOVIE CAPTIONS

FIGURE S1 - Region I of the force curve for tether extration in a NIH 3T3 control cell. Grey curve is the experimental curve and black curve is the fit using the theoretical model. With this theoretical model we can determine the G_0 parameter of the cell. The fit starts beyond the region that might be contaminated by sliding. In this curve, the G_0 parameter is 977Pa.

FIGURE S2 – Beads of different size yield the same tether force values in Fibroblast NIH 3T3 cells. Bright field images with ImageJ shadow north processing filter applied showing the extracted tethers (indicated with arrows) using a 0.53μm radius bead (a) and a 1.52μm radius bead (b). (c) Results for tether force using 0.53μm radius beads (gray bar) and 1.52 μm radius beads (white bar). Standard errors were used as error bars. At least 20 different experiments for each situation ($p > 0.16$ *means no significant statistical differences using the t-test*). Scale bars are 10μm.
– Bead size does not affect the presence of F-actin inside tethers pulled from Fibroblast NIH 3T3 cells. (d) actin staining for phaloidin-FITC. (e) Zoom showing the presence of F-actin in the extracted tethers. (f) brightfield/fluorescence merge image of the tethers showing the presence of F-actin in tethers pulled with beads of different sizes. (g) Plot representing the green level fluorescence (GL) of a tether pulled with the 0.53μm radius bead (white bar) and with the 1.52μm radius bead (light gray bar), normalized by the green level fluorescence inside the cell ($GL_{(cell)}$) (dark gray bar). Scale bars are 10μm.

FIGURE S3: (a) brightfield/fluorescence merge image of the tether showing the presence of F-actin in tethers pulled from 3T3 cells. (b) actin staining with phaloidin-FITC. (c) zoom showing the presence of F-actin in the extracted tethers. Scale bar is 10 μm.

MOVIE S1: Tether extraction time-lapse experiment. A polystyrene microsphere $(a = 1.52 \pm 0.02 \mu m)$ was attached to a 3T3 cell surface using the optical trap. After that, the sample was moved with a constant velocity (0.071±0.002μm/s) keeping the trap turned on. The movie shows the trajectory of the microsphere. The vertical white line indicates position Vt for zero force on the trap, so that $\Delta\rho$ is the distance between the microsphere center and this line. As the sample moves a distance d, the white line moves away from the initial position (indicated by the black line).Video acquisition was performed at 2 frames/second. The total duration of this specific experiment was 198s. Scale bar: 10μm.

FIGURES

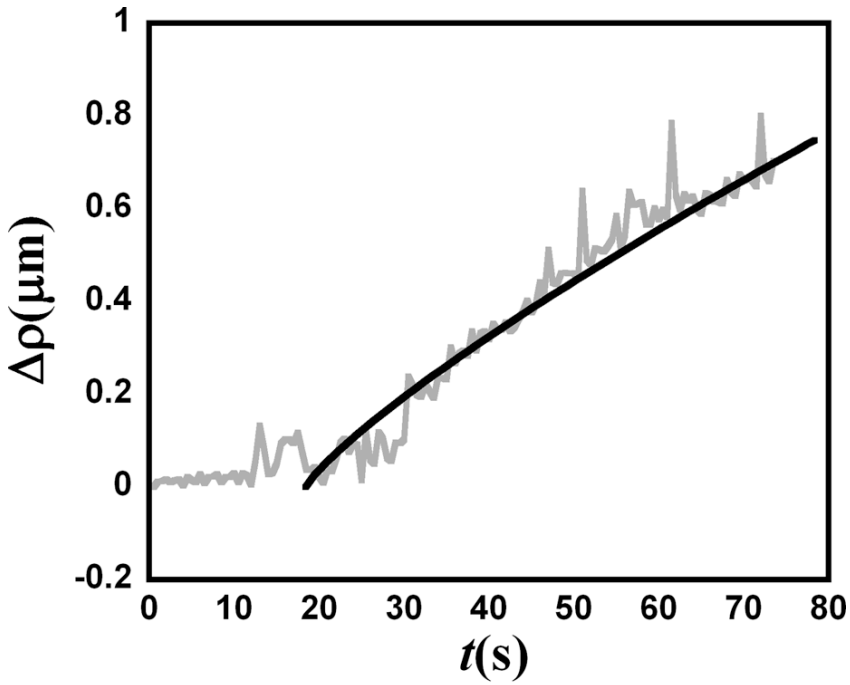

Pontes *et. al* FigS1

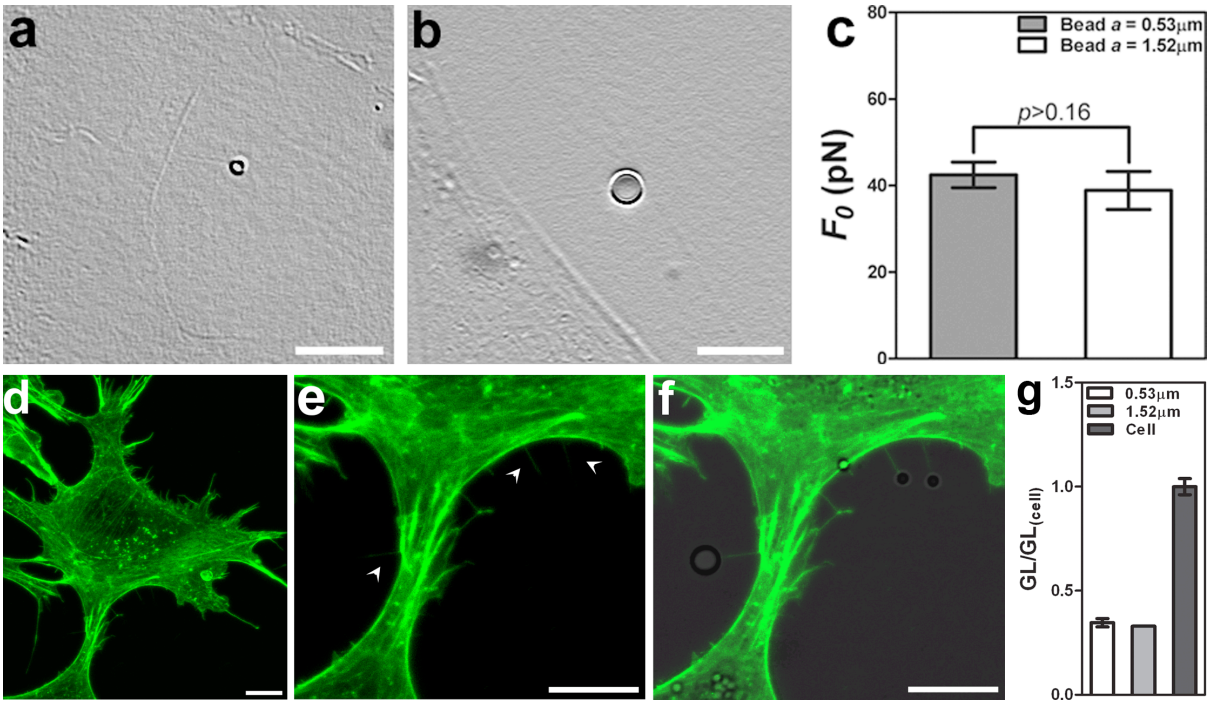

Pontes et al. Fig. S2

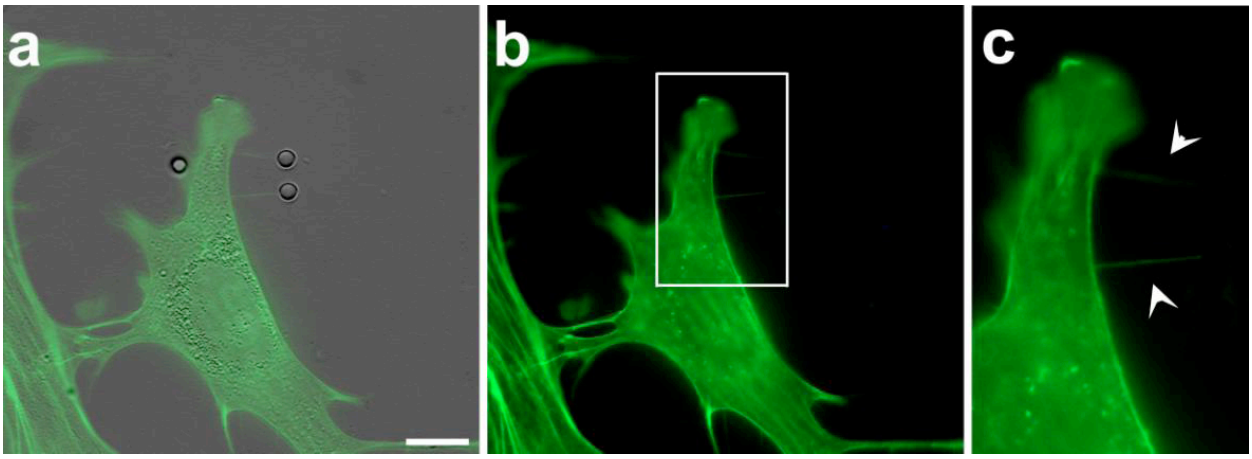

Pontes et al. Fig. S3